symmetry

MDPI

Article

Analysis of the Propane Price Oriented Weighted Network Based on the Symbolic Pattern Representation of Time Series

Guangyong Zhang [1], Yan Zhu [2], Jiangtao Yuan [1] and Zifang Qu [3,*]

[1] Department of General Education, Wuxi University, Wuxi 214105, China; zhanggy_ujs@126.com (G.Z.); jtyuan@hpu.edu.cn (J.Y.)
[2] School of Digital Economics and Management, Wuxi University, Wuxi 214105, China; zhu2099789759@163.com
[3] School of Mathematics and Information Science, Shandong Technology and Business University, Yantai 264005, China
* Correspondence: quzifang@163.com

Abstract: As an essential chemical raw material and a cost-effective energy product, fluctuations in propane price has garnered significant attention in the energy market. This paper processes the original time series using a coarse-grained method and employs symbolic representation combined with the sliding window technique to represent fluctuation modes as nodes within a network. The weight and direction of the edges among the nodes are determined by the number and direction of the conversions among the modes, thereby mapping the original sequence of the propane price into the propane price oriented weighted network (PPOWN) by the symbolic patterns, which is an asymmetric network that has evolved from the symmetric network based on symmetry theory. The results indicate that the core fluctuation state of the PPOWN is concentrated in the first 0.96% of the nodes, exhibiting scale-free network characteristics and dynamic asymmetry. Nodes with greater strength are more closely interconnected, but not all early-appearing nodes possess great strength. The PPOWN demonstrates a short-range correlation ($\overline{L} = 8.5405$) and a highly linear growth trend in the cumulative time interval of the new nodes. Additionally, the nodes of the PPOWN display low betweenness, clustering coefficient, and strength, which significantly differ from the random and chaotic networks. The presence of these lower-strength nodes often signifies that the market is undergoing a transformation or transition period. By identifying and analyzing these nodes, subsequent propane price fluctuations can be predicted more effectively, enhancing market responsiveness.

Keywords: propane price; oriented weighted network; coarse-grained method; sliding window; strength; clustering coefficient

check for updates

Academic Editors: Ming Li and Calogero Vetro

Received: 28 April 2025
Revised: 21 May 2025
Accepted: 23 May 2025
Published: 25 May 2025

Citation: Zhang, G.; Zhu, Y.; Yuan, J.; Qu, Z. Analysis of the Propane Price Oriented Weighted Network Based on the Symbolic Pattern Representation of Time Series. *Symmetry* **2025**, *17*, 821. https://doi.org/10.3390/sym17060821

Copyright: © 2025 by the authors. Licensee MDPI, Basel, Switzerland. This article is an open access article distributed under the terms and conditions of the Creative Commons Attribution (CC BY) license (https://creativecommons.org/licenses/by/4.0/).

1. Introduction

As an important chemical raw material and environmentally friendly source of energy, the price fluctuation of propane not only directly affects the supply and demand balance of the energy market but also has a profound impact on global economic structure and the stability of the industrial chain [1]. In recent years, the transformation of the energy structure and the intensification of geopolitical changes have led to significant price fluctuations in propane [2], which exhibit highly nonlinear and complex characteristics. Traditional statistical methods face considerable challenges in analyzing the underlying dynamic mechanisms of these fluctuations. How to accurately capture the fundamental patterns of the price fluctuations and predict market trends [3] has become a significant focus of interest in both academia and industry.

Early studies primarily utilized time series models to analyze the volatility characteristics of propane prices. For instance, the GARCH model, proposed by Hamilton [4], is extensively utilized in the energy market. It effectively captures volatility clustering and leverage effects, thereby revealing the conditional heteroskedasticity of price fluctuations. Pindyck [5] integrated supply and demand elasticity with inventory dynamics into the analytical framework, highlighting that propane prices are significantly influenced by interconnection with the crude oil market, and that fluctuations in this market had substantial cross-market contagion effects. Dias et al. [6] conducted a comprehensive analysis of oil, gas, and electricity prices in the U.S. market using a multi-transformation model that effectively captured the typical characteristics of energy prices. Soohyeon et al. [7] found that the decline in ethane price, attributed to the U.S. shale gas boom, resulted in lower ethylene prices and higher propylene prices, while propane continued to be the primary factor influencing the latter. Nazioglu et al. [8] examined the existence of volatility transmission between oil prices and financial pressures using a volatility spillover test. Moul and Miller [9] used instrumental variables to estimate the monthly propane demand and (inverse) supply equations, and believed that the propane distributors who usually adopt a low-price strategy have temporary market dominance. Zhang et al. [10] employed various econometric models to empirically examine the price discovery and risk transfer functions within the crude oil and gasoline futures markets. According to the wavelet transform method, Hung [11] examined the short-term and long-term dependencies between crude oil and propane prices during the period 2006–2018, and found that there was a strong correlation between the crude oil and propane series in the short and medium term, while, in the long term, propane returns had a unidirectional impact on the crude oil market. In summary, numerous scholars both domestically and internationally have conducted systematic research on issues related to energy price systems using various methodologies. They have established many practical models to examine the transmission relationships between energy prices and their associated factors, as well as to predict future trends and volatility in energy prices. However, traditional research methods for analyzing energy price fluctuations primarily rely on the development of various econometric models to explain the causes and mechanisms behind oil price fluctuations. It is important to note that the energy price system is fundamentally a complex, nonlinear, and non-stationary system. Traditional approaches seldom address how to construct complex network analysis models for energy prices or how to explore the intricate characteristics of the energy price system. In recent years, complex networks have emerged as a research hotspot, with the central idea of interpreting the connections between different components of the system as complex networks to gain a deeper understanding of the essence of real-world systems.

In order to address the limitations of traditional models, the complex network theory has increasingly been integrated into energy market research [12,13]. Chiroma et al. [14] proposed an integration of CRT-RVFLN-SVM (Classification and Regression Tree (CRT), Random Variable Function Link Neural Network (RVFLN), and Support Vector Machine (SVM)) to enhance the robustness and effectiveness of propane price estimation. Emmert-Streib and Dehmer [15] proposed mapping financial time series to network nodes and quantifying the transformation rules of market states through topological indicators, such as degree distribution and clustering coefficient. This method has led to significant breakthroughs in stock market research. For instance, Mantegna and Stanley [16] utilized the minimum spanning tree algorithm to uncover the correlation structure of asset prices. Huang et al. [17] utilized a GA-LightGBM model with genetic algorithm-optimized parameters to construct an oriented weighted network and investigated whether the centrality of the stock network aids in predicting company performance. In recent years, He and Chen [18] applied symbolic dynamics to the construction of crude oil price networks and

discovered that key nodes have a warning effect on systemic risks, thereby providing a methodological reference for propane research.

Symbolic methods are being increasingly utilized in economics [19]. Narayan et al. [20] examined five distinct types of oil futures contracts and analyzed the clustering of price fluctuations. Daw et al. [21] proposed that coarse-graining can effectively reduce noise and extract the semantic features of time series data, and the results confirmed the superiority of symbolic processing in exchange rate forecasting. Wu et al. [22] converted time series into price graphs and used graph embedding techniques to extract meaningful structural features. Zhou et al. [23] further integrated the sliding window technique with the hidden Markov model, successfully predicting the mutation points of gold prices, which makes evident that symbolic network methods offer innovative tools for market forecasting and risk management by uncovering global interaction structures and the dynamics of the key nodes. Cheng et al. [24] introduced a multi-modality graph neural network (MAGNN) for financial prediction using heterogeneous graphs, and the graph-centric view of market dynamics in their paper conceptually aligns with the method used in this paper.

At present, research on energy price fluctuations primarily focuses on time series analysis, volatility modeling, and the identification of influencing factors. For instance, researchers employ the GARCH model to characterize the clustering of energy price fluctuations [25] and utilize cointegration to examine the dynamic relationships among international crude oil, natural gas, and coal price indices [26]. However, these methods are often limited to local feature extraction and struggle to reveal the global interactive network and dynamic evolution of price fluctuations. At the same time, the successful application of complex network theory in financial time series analysis offers a novel perspective for energy market research. By mapping price series into network nodes and edges, researchers can systematically analyze the transition paths of market conditions, the influence of key nodes, and the topological robustness of the network. Despite this, existing research has primarily concentrated on oil prices [27] or heating oil prices [28]. In contrast, the exploration of propane price fluctuation networks remains inadequate, and there is a notable absence of the targeted methodologies regarding symbolic representation, the dynamic weight definition, and the core node identification. Choi and Kim [29] present a graph-based risk analysis framework that considers inflation-adjusted dependence in global financial markets, and their approach to network construction and entropy-based evaluation offers conceptual support for your symbolic network methodology.

Inspired by symmetry theory, this study conceptualizes price fluctuations as a dynamic symmetry-breaking process. And the sliding window technique introduces time translation symmetry, ensuring that the generation process of the fluctuation mode adheres to the translation invariance constraint of the time series, and this symmetry framework not only reduces the dimensionality of the data but also preserves the essential dynamic characteristics of price fluctuations. Therefore, this paper constructs a PPOWN based on a specific framework and explores the network's topological structure. This study presents three innovative contributions as follows.

(1) We transform the fluctuation sequence of propane price into a feature set consisting of five symbols {R, r, e, f, F}, which differs from the previous literature [30,31] that utilized three symbols {Y, O, N}. This transformation method more effectively captures the complexity of the propane price fluctuation.

(2) A PPOWN is constructed based on the fluctuation sequence and analyzed for comparison, which confirms that the PPOWN is a scale-free network.

(3) In constructing the network, the time factor was taken into account, and the evolution of nodes over time was examined. This approach not only identified important nodes but also investigated the distribution characteristics of the appearance times of these

significant nodes. This method not only overcomes the limitations of traditional models in effectively representing nonlinear relationships, but it also quantifies the significance and clustering characteristics of fluctuation patterns by utilizing topological indicators such as node strength, betweenness centrality, and clustering coefficients.

The framework structure of this paper is organized as follows (as illustrated in Figure 1): Section 2 introduces the data sources, data processing methods, and the model construction process; Section 3 introduces the topological properties of the PPOWN; Section 4 provides a comprehensive discussion that integrates the previous sections; and, finally, the summaries and insights are given in Section 5.

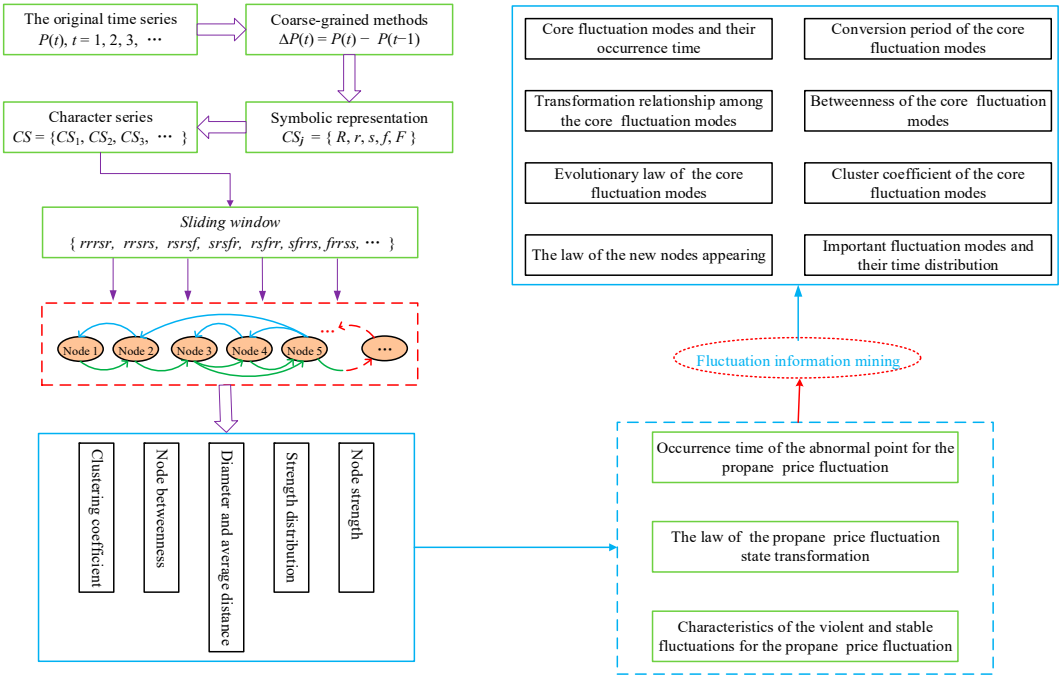


Figure 1. The framework structure of this paper.

From the research framework of this paper, the study can be divided into three levels. First, we convert the propane price fluctuation series into a symbolic sequence. Next, we construct a PPOWN based on the transformations among different fluctuation modes, and we discuss the topological properties of this network. Subsequently, we derive the dynamic characteristics of the propane price fluctuation model from the topological properties of the PPOWN. Following this, we analyze the volatility behavior characteristics of propane price based on the dynamic features of the fluctuation model. Finally, we examine the linear characteristics of the cumulative time of outliers in the propane price fluctuation process and identify the time distribution characteristics of significant patterns that emerge during this process.

2. Data and Model

2.1. Data Source and Processing Method

The propane daily closing spot prices from the U.S. Energy Information Administration (9 July 1992 to 22 July 2024) are selected for this study, the fluctuation trends of which are shown in the Figure 2 (https://www.eia.gov/dnav/pet/pet_pri_spt_s1_d.htm, Accessed on 28 July 2024.).

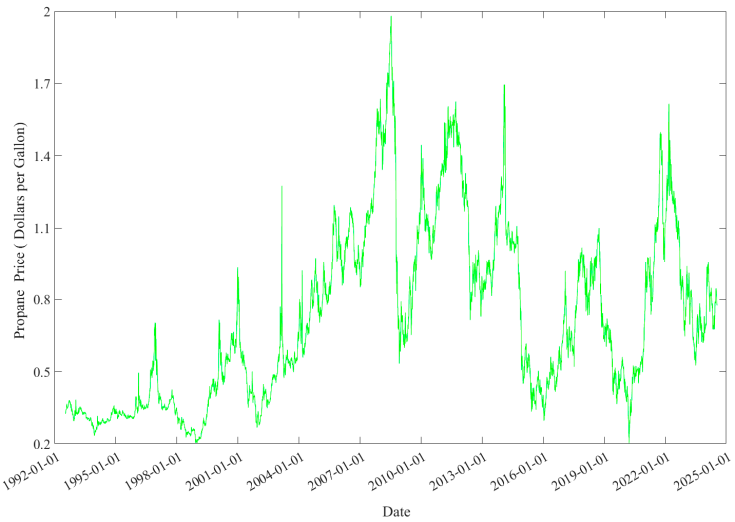


Figure 2. The fluctuation trend of the propane price.

Fluctuations in propane prices are a primary concern for investors. Therefore, this paper designates a propane price time series as $P(t), t = 1, 2, \ldots, n$. For a continuous propane price series, the price fluctuation series is defined as $P(t)$, where $P(t)$ represents the current price and $P(t-1)$ the previous price. The coarse-grained time series $\Delta P(t)$ and M is calculated as the Formulas (1) and (2), respectively.

$$\Delta P(t) = P(t) - P(t-1), \tag{1}$$

$$M = \frac{\sum_{t=1}^{n-1} |\Delta P(t)|}{n-1}, \tag{2}$$

where $\Delta P(t)$ is the coarse-grained time series, M is the average of the absolute values of the coarse-grained time series. When $\Delta P(t) > M$, the propane price is considered to have risen sharply; when $0 < \Delta P(t) \leq M$, the propane price is considered to have risen slowly; when $M = 0$,the propane price is considered to have fluctuated steadily; when $-M \leq \Delta P(t) < 0$, the propane price is considered to have fallen slowly; when $\Delta P(t) < -M$, the propane price is considered to have fallen sharply. According to the coarse-grained method, we have achieved the processing of the original time series, which provides a prerequisite for the symbol representation in Section 2.2.

2.2. Symbolization of the Coarse-Grained Time Series

In order to reveal the fluctuation patterns of propane price, five distinct characteristics (i.e., R, r, s, f, F) are selected to represent the fluctuation state of the coarse-grained time series. The coarse-grained time series is then converted into a character sequence. Next, the size relationship between $\Delta P(t)$ and M is mapped to their corresponding characters, resulting in a character sequence that represents the price of propane. The corresponding character sequence is shown in Formula (3).

$$CS_j = \begin{cases} R, \ \Delta P(t) > M \\ r, \ 0 < \Delta P(t) \leq M \\ s, \ M = 0 \\ f, \ -M \leq \Delta P(t) < 0 \\ F, \ \Delta P(t) < -M \end{cases}, \tag{3}$$

where $j = 1, 2, \ldots, n-1$, and R, r, s, f, F respectively represent the sharp rising, slow rising, stable fluctuation, slow falling and sharp falling of the propane price. Therefore, the propane price fluctuation sequence is converted into the corresponding character sequence:

$$CS = \{CS_1, CS_2, CS_3, \ldots\ldots\}, CS_j \in (R, r, s, f, F).$$

The method renders the analysis of the coarse-grained symbol sequence equivalent to the research of the corresponding time series. Taking the 101st to 150th of the coarse-grained sequences of the propane price sequence as an example, the results of converting these coarse-grained sequences into a character sequence are illustrated in Figure 3. Through the symbolic pattern representation of the coarse-grained time series, the original time series are converted into the symbolized time series, that is the symbolic sequences, which provides a foundation for the construction of the fluctuation modes in the next section.

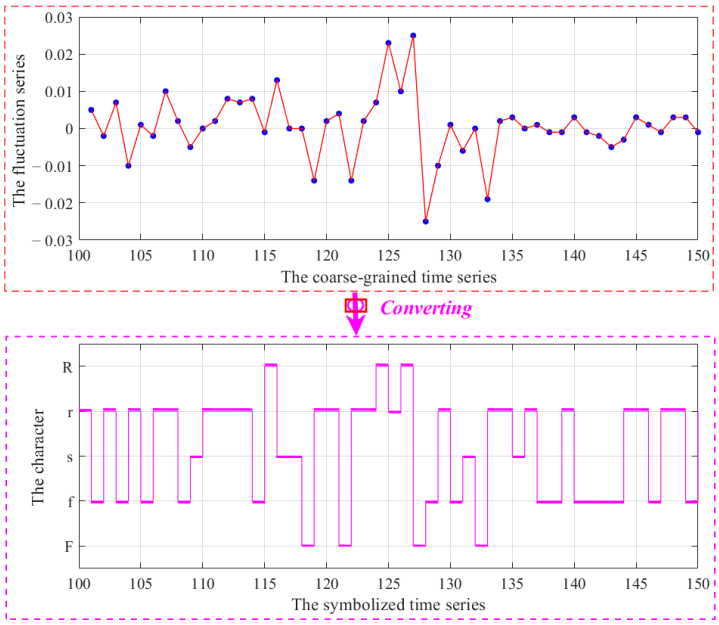


Figure 3. The coarse-grained time series characterization.

2.3. Constructing the PPOWN

In the process of converting the propane price sequences into a string sequence, selecting the appropriate time interval is a crucial step. This choice not only determines the duration represented by each data point in the sequence but also influences the precision and informational content of the data. Consequently, it affects the observable price dynamics and patterns. In addition, the proportions of each character and the correlations between characters will also vary. For example, when considering a length of five characters, the proportions are illustrated in Figure 4.

In Figure 4, the data presented in blue font represents the horizontal axis, while the vertical axis denotes various character types, and the data displayed in red font indicates the proportion of five distinct characters $\{R, r, s, f, F\}$ within the network. According to the availability and completeness of the daily price data, this paper employs a five-character sequence as a fluctuation mode to ensure consistency between theoretical analysis and actual time intervals. The data is slid with a step size of one day. Take the PPOWN as an example, as illustrated in the CS column in Table 1.

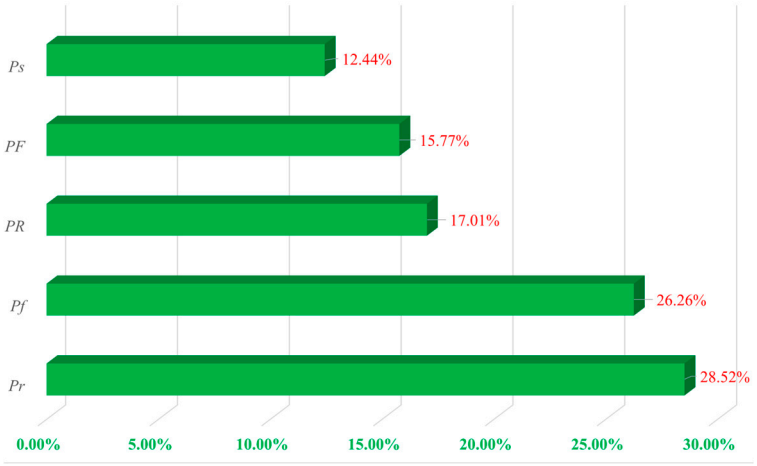


Figure 4. The percentage of different characters.

Table 1. The process of constructing the PPOWN.

Time Series	Price Series $P(t)$	Coarse-Grained Series $\Delta P(t)$	*CS*	Fluctuation Modes
9 July 1992	0.324			
10 July 1992	0.328	0.004	r	
13 July 1992	0.329	0.001	r	
14 July 1992	0.334	0.005	r	
15 July 1992	0.334	0.000	s	
16 July 1992	0.341	0.007	r	rrrsr
17 July 1992	0.341	0.000	s	rrsrs
20 July 1992	0.341	−0.001	f	rsrsf
21 July 1992	0.344	0.001	r	srsfr
22 July 1992	0.344	0.003	r	rsfrr
23 July 1992	0.344	0.000	s	sfrrs
24 July 1992	0.345	0.000	s	frrss
27 July 1992	0.353	0.001	r	rrssr
28 July 1992	0.341	0.008	r	rssrr
• • •	• • •	• • •	• • •	• • •
16 July 2024	0.785	−0.010	f	FfsFf
17 July 2024	0.783	−0.002	f	fsFff
18 July 2024	0.781	−0.002	f	sFfff
19 July 2024	0.775	−0.006	f	Ffff
22 July 2024	0.776	0.001	r	ffffr

The sliding windows

Based on the continuous symbol sequence, the sliding window method is utilized to divide the symbol sequence into the fluctuation modes, as the number of propane trading days is 5 days per week (there is no trade on weekends.). Accordingly, the fluctuation states of the propane price on these days are denoted by five symbols, so the length of the sliding window is five. Meanwhile, if the propane price is the daily price, then the step size of the sliding window is one. There is some overlap among these fluctuation modes, with the former serving as the foundation for the subsequent mode. Consequently, the fluctuation modes exhibit the characteristics of memory and transitivity.

Since the fluctuation mode is established through data sliding, the previous fluctuation mode serves as the foundation for the formation of the next fluctuation mode, and the fluctuation modes are both transitive and directional. Therefore, by considering each fluctuation mode as a node within the network and interpreting the conversion direction between the fluctuation modes as the direction of the network edge, we can establish the weight and direction of the edges between the network nodes based on the number of conversions. If the modality changes from the current state to the next moment, an edge is created between the two modalities, and the edge weight is increased by one. The direction of both edges is from the current modality to the next modality. However, if the current modality remains the same as the modality at the next moment, the network remains unchanged. By repeating this cycle, an oriented weighted network of the propane price fluctuations can be constructed. The construction process is illustrated in Table 1.

In Table 1, the fluctuation modes change continuously as the sliding window moves, resulting in a total of 8032 fluctuation modes for the propane price (including the duplicate modes). These fluctuation modes serve as the nodes in the network (the first node corresponds to the date 16 July 1992 and is labeled as 'rrssr'). The duplicate fluctuation modes are merged, ultimately yielding 2289 distinct propane price fluctuation modes. In summary, the PPOWN is established based on the length and step size of the sliding window, comprising 2289 nodes. As for the difference between this paper and the references [30,31], we mainly expanded the fluctuation pattern from the original three fluctuation characters to five fluctuation characters, and the specific differences in the improvements are shown in Table 2.

Table 2. Differences between this paper and the references [30,31].

Comparison Object	References [30,31]	This Paper
Number of the fluctuation	3	5
Name of the fluctuation character	Y, O, N	R, r, s, f, F
Length of the fluctuation mode	5	5
Number of the fluctuation mode	$3^5 = 243$	$5^5 = 3125$
Name of the fluctuation mode	{YONYN}	{RFrfs}

Where the characters Y, O and N respectively represent three fluctuation states: rising, staying constant, and falling. The characters R, r, s, f, F represent the sharp rising, slow rising, stable fluctuation, slow falling and sharp falling, respectively. According to the number of the fluctuation character, we can find that the fluctuation state in this paper is not only more abundant compared to the references [30,31], but also more detailed in its characterization. As for the number of the fluctuation mode, the method proposed in this article allows for the possibility of up to 3125 different fluctuation modes, compared to only 243 modes achievable with methods found in the literature [30,31]. This approach in this paper not only exhibits greater complexity but also offers more precise descriptions of price fluctuations.

2.4. Definition and Calculation Formula of the Indicators

Through the aforementioned network construction methods, the PPOWN can be established. This section will present the calculation formulas for various static indicators within the oriented weighted network, including the strength, network diameter, average path length, betweenness, and clustering coefficient. This is a crucial step in quantitative analysis, as it aids in understanding and explaining network characteristics, predicting and optimizing network performance, achieving standardization and comparability, and fulfilling the requirements of scientific research and practical applications.

2.4.1. The Strength and Distribution

The strength of the node in complex networks is a crucial property. This metric not only indicates the connections between a node and other nodes but also represents the weights of the edges connecting them. In other words, strength is a weighted version of degree, defined as the sum of the weights of all edges associated with a given node. The strength of the node in a directed network is categorized into input strength and output strength, and the calculation formula is shown in Formula (4) [32].

$$s_i^{in} = \sum_{j=1}^{N} \omega_{ji},\ s_i^{out} = \sum_{j=1}^{N} \omega_{ij}. \tag{4}$$

The input strength of the node v_i indicates the times of other nodes are transformed into the node v_i, while the output strength of the node v_i reflects the times of the node v_i are transformed into other nodes. s_i^{in} and s_i^{out} represent the input and output strengths of the node, respectively. ω_{ji} denotes the weight of the edge connecting node v_j to v_i; if $w_{ji} = 0$, it signifies that there is no connection from the node v_j to v_i. The larger the strength value of a node, the greater its significance within the network, which may correlate with a higher number of interaction relationships. Nodes with higher strengths are considered central to the network, while those with lower strengths are typically peripheral or terminal nodes. Nodes with elevated strengths are often referred to as important nodes. By measuring the strength of nodes, one can visually assess their local connectivity within the network. For instance, in a social network, a higher strength of a node indicates that the corresponding individual has more friends, reflecting greater interpersonal communication.

The definition of the distribution for the strength of the node is presented in Formula (5).

$$p(s) = \frac{s_i}{N}. \tag{5}$$

where s_i represents the node strength, and N denotes the sum of the strengths of all nodes. A higher node strength and strength distribution of a mode indicate that it is more frequently transformed into other modes (including the current mode), which suggests a greater likelihood and significance of its presence within the network. Furthermore, if the strength distribution $p(s)$ of the node in a network can be fitted to the power law distribution described in Formula (6), it signifies that the network is a scale-free network. By taking the logarithm of both sides of Formula (6), Formula (7) can be derived.

$$p(s) = Cs^{-\gamma}, \tag{6}$$

$$\ln p(s) = \ln C - \gamma \ln s. \tag{7}$$

where C represents the proportional constant, and γ denotes the power exponent. A larger value of the power exponent indicates a stronger power law distribution within the network.

According to the construction method of the PPOWN outlined in Section 2.3, the nodes are connected in chronological order. Consequently, the input strength and output strength of the nodes are identical, with the exception of the first and last nodes. For the sake of convenience in calculation and description, the following text will focus solely on the output strength of the nodes, which will be referred to simply.

2.4.2. The Diameter and Average Path Length

A simple path between two nodes v_i and v_j in a network that traverses the least number of distinct edges is referred to as a geodesic. The number of edges d_{ij} in the geodesic is termed the distance between nodes v_i and v_j. The diameter D of the network

is defined as the maximum value among all distances d_{ij}, and the calculation formula is presented in Formula (8).

$$D = \max_{1 \le i,j \le N} d_{ij}. \tag{8}$$

The average path length L represents the average distance between any two nodes in a network [31,33,34]. For a directed network, the calculation formula L is presented in Formula (9).

$$L = \frac{1}{N(N-1)} \sum_{i \neq j} d_{ij}. \tag{9}$$

where N represents the number of the nodes in the network.

2.4.3. The Betweenness

In the network, the busiest node—defined as the node that plays the most significant role in connectivity—occupies a more important position within the network. To assess the significance of a node, its degree can certainly serve as an indicator, but it is not the sole measure of importance. Therefore, we need to define an additional measurement indicator, specifically betweenness [34–37], which is a global feature that reflects the influence and role of a node or edge within the entire network. The shortest path between non-adjacent nodes v_j and v_l in the network will traverse through several intermediate nodes. If the node v_i is included in many other shortest paths, it indicates that this node holds significant importance, and the influence can be quantified by the betweenness, denoted as B_i. In a directed network, the betweenness B_i of the node is defined as presented in Formula (10).

$$B_i = \sum_{j \neq l \neq i} [N_{jl}(i) / N_{jl}]. \tag{10}$$

where N_{jl} represents the number of shortest paths from node v_j to node v_l, and $N_{jl}(i)$ represents the number of shortest paths from the node v_j to v_l that pass through the node v_i. The betweenness of the node v_i can be defined as the proportion of the total number of shortest paths in the network that pass through this node. Betweenness primarily measures the extent to which each node in a network lies on the shortest paths between other nodes. Since information traverses each node with equal probability, the number of nodes involved in each information propagation is directly proportional to the number of nodes on the shortest path that includes the given node. A node that lies on the shortest path between many other nodes is considered significant. In a network, a node with higher betweenness centrality is more active, indicating that it facilitates greater connectivity. Consequently, such a node occupies a relatively important position within the network.

2.4.4. The Clustering Coefficient

According to references [38,39], the clustering coefficient C_i of the node v_i in an oriented weighted network is defined as shown in Formula (11).

$$C_i = \frac{1}{s_i(k_i - 1)} \sum_{j,k} \frac{\omega_{ij} + \omega_{ik}}{2} a_{ij} a_{jk} a_{ik}. \tag{11}$$

where ω_{ij} and ω_{ik} represent the edge weights of the edges between the nodes v_i and v_j, and the nodes v_i and v_k, respectively, S_i represents the strength of the node v_i (where $s_i = \sum_j \omega_{ij}$), k_i is the degree of the node v_i, and $\sum_{k>j} a_{ij} a_{jk} a_{ik}$ represents the total number of triangles in the network that contain the node v_i. The clustering coefficient of a node primarily reflects the degree of connectivity among its neighboring nodes, specifically the probability of edges existing between these neighbors. This metric serves as an indicator

of the network's cohesiveness and illustrates how a node is integrated within its local environment. If $C_i = 1$, it signifies that all neighboring nodes are interconnected, while $C_i = 0$ indicates relatively sparse connections within the network. Intuitively, the clustering coefficient can be understood as the proportion of a node's neighbors that are themselves interconnected. A higher clustering coefficient suggests a greater likelihood of interactions among a node's neighbors, which may indicate the presence of a functional module within the network.

The average clustering coefficient indicates the average probability that two nodes connected to a common node in a network are also directly connected to each other, which is commonly used to characterize the local structural properties of the network. The clustering coefficient is averaged across the entire network, resulting in the average clustering coefficient, as demonstrated in Formula (12).

$$C = \frac{1}{N}\sum_{i=1}^{N} C_i. \tag{12}$$

Obviously, $0 \leq C \leq 1$. If $C = 0$, it happens only when the clustering coefficients of all nodes in the network are equal to 0; while $C = 1$ only occurs when the clustering coefficients of all nodes in the network are equal to 1. In this case, the network is globally coupled, meaning that any two nodes in the network are directly connected.

3. Empirical Analysis

By constructing the PPOWN, we aim to elucidate the patterns of these fluctuations. This approach not only offers a comprehensive understanding of the market dynamics and the underlying causes of the price changes but also enables the evaluation of propane price variations at different time points. Consequently, it assists companies in optimizing resource allocation on a global scale. Furthermore, this analysis provides scientific decision-making support for companies in production, procurement, sales, and other areas, thereby enhancing their competitiveness in a complex market environment. This section will analyze the PPOWN, focusing on key indicators such as node strength and distribution, the regularity of new node emergence, the node conversion cycle, node betweenness, and the clustering coefficient.

3.1. Strength and Distribution of the Nodes

By recognizing the significance of nodes and the strength of connections within the PPOWN, companies can effectively adjust their production and inventory strategies in a timely manner when confronted with market fluctuations. This proactive approach helps to mitigate risks and capitalize on market opportunities. In order to further elucidate the temporal distribution characteristics and power-law distribution properties of significant nodes within the PPOWN, this section examines the node strength and distribution characteristics of the PPOWN, as illustrated in Figure 5.

The strength and distribution of nodes illustrate the correlation among the fluctuation modes of propane price. A greater strength of nodes within a modality indicates a higher frequency of transformation into other modes (including the current mode) and an increased probability of occurrence within the network. The left axis in Figure 5 represents the strength of the corresponding node, the right axis illustrates the cumulative strength distribution of the nodes, and the horizontal axis denotes the corresponding nodes. As shown in Figure 5, most nodes in PPOWN display low strength, whereas only a few nodes demonstrate high strength, which indicates that the likelihood of most nodes appearing in the PPOWN is relatively low. Meanwhile, the distribution of strength reflects that the PPOWN appears the typical characteristics of a scale-free network.

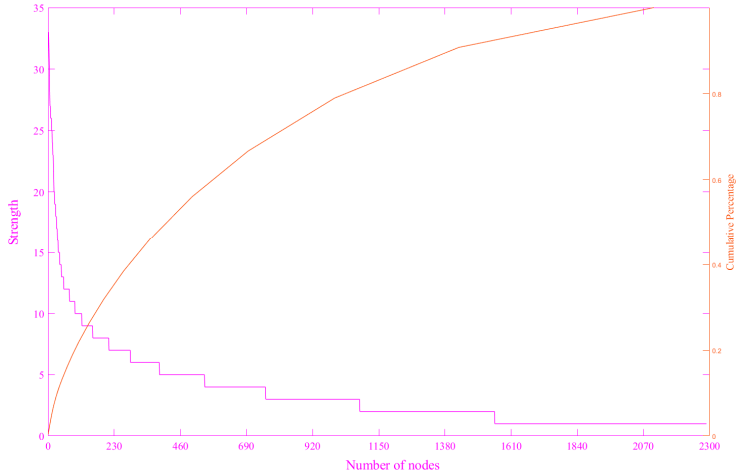


Figure 5. The strength and distribution of the nodes in the PPOWN.

In addition, there are 2289 nodes in the PPOWN. Among these, 22 nodes have a strength greater than or equal to 20, resulting in a total degree of 572. These nodes account for 7.18% of the overall strength, which is 7963. In other words, 0.96% of the nodes contribute to 7.18% of the total strength, as illustrated in Table 3.

Table 3. Statistics of the important nodes in the PPOWN.

Total Number of the Nodes	Number of Important Nodes (*Strength*≥20)	The Proportion of the Important Nodes	The Proportion of the Sum of the Important Node	Average Contribution Rate of Connections Among Important Nodes
2289	22	0.96%	7.18%	55.77%

In the PPOWN, the average contribution rate of the connections between the important nodes and node strength is 55.77%. The result indicates that the PPOWN exhibits clear positive correlation characteristics. Specifically, nodes with a large strength tend to connect with other nodes of high strength. From the analysis above, it is evident that, while the transitions between fluctuation states of the propane price occur frequently and exhibit considerable complexity, the initial 0.96% of the nodes effectively represent the core fluctuation state of the propane price, which suggests that the future fluctuation state of the propane price is likely to resemble the fluctuation state observed during a specific period in the past. Therefore, by identifying the fluctuation patterns of the initial 0.96% of the nodes and the relationships between their transformations, we can provide an approximate description of the fundamental characteristics of propane price.

The strength of the node can reflect the influence or importance of a node within the entire network to a certain extent. Therefore, we examined the nodes with a node strength greater than or equal to 20 in the PPOWN. We obtained the node names, strengths, and appearance times (as shown in Figure 6). In this figure, the red lines indicate positive direction, the blue lines indicate reverse direction, the characters represent the names of the nodes, and the numbers on the lines between nodes indicate the weights.

In Figure 6, it is evident that, from the moment significant nodes emerge, the PPOWN reveals that nodes with high point strength are closely interconnected. While the nodes with high point strength tend to be those that appeared earlier, it is important to note that their earlier appearance does not guarantee a high point strength. In the PPOWN, the 22 nodes with a node strength of 20 or greater range from the 12th to the 182nd nodes in the network. Among these, the node 'ffrrr', which has the highest strength of 33, first appeared

on 18 August 1992, making it the 24th node to be introduced in the PPOWN. Among the first 182 nodes in the PPOWN, 7 nodes exhibit a strength of one. The earliest node is 'rfssF', which was introduced on 30 November 1992. This node is the 79th to appear in the PPOWN. It is evident that the nodes appearing early in the PPOWN do not necessarily possess strong point strength.

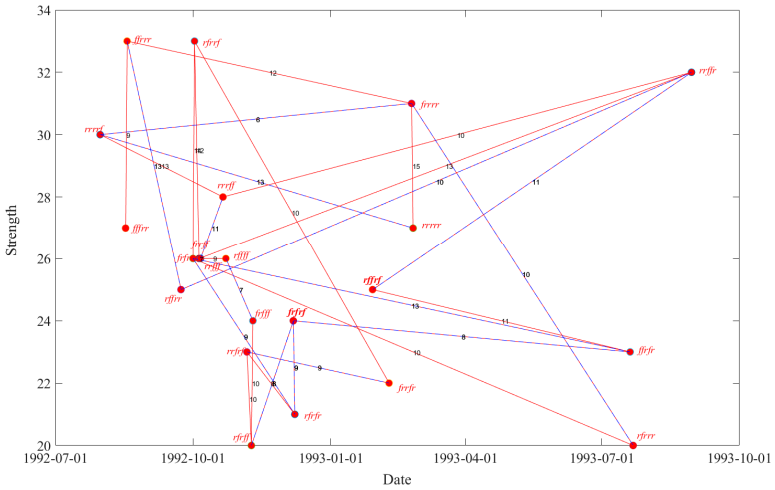


Figure 6. The time when the important nodes appear in the PPOWN.

According to the Formulas (5)–(7), the double logarithmic representations of the node strength distribution for the PPOWN are presented below, as illustrated in Figure 7.

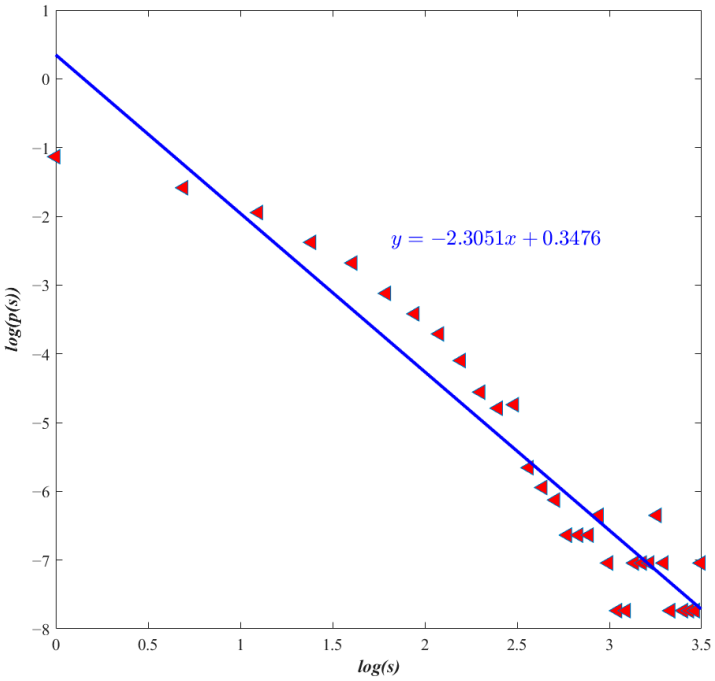


Figure 7. The double logarithmic graph of the strength for the node in the PPOWN.

In Figure 7, the red triangles represent the fitted data points, specifically the logarithm of the strength and its corresponding proportion. Figure 7 illustrates that, in the PPOWN, the majority of the nodes exhibit a low point strength, while only a small number of the nodes demonstrate high point strength. Using the least squares method for straight line fitting, the double logarithmic curve of the node strength in the PPOWN is subjected to linear regression. The resulting regression equation is denoted as $y = -2.3051x + 0.3476$,

and the correlation coefficient of the trend line along with the power exponent is presented in Table 4.

Table 4. The fitting parameters of the strength distribution in the PPOWN.

***F*-Value**	***p*-Value**	γ	R^2
359.9336	0.0000 ***	2.3051	0.9231

Notes: *** expresses at a significant level of 1%.

As illustrated in Table 4, the results demonstrate a high degree of credibility, indicating that the PPOWN follows a power-law distribution overall. The result also indirectly suggests that the PPOWN mentioned above is a scale-free network. For a scale-free network, a higher degree of power-law distribution corresponds to a larger power exponent. The power-law exponent (γ) of the PPOWN is 2.3051, the value of which indicates that the PPOWN exhibits high complexity and regularity, which indirectly reflects the intricate intrinsic dynamic characteristics of the network.

3.2. Regularity of the New Node Appearance

According to the PPOWN, we begin by studying the cumulative time intervals of new nodes that appear in the network to analyze their occurrence patterns, as illustrated in Figure 8.

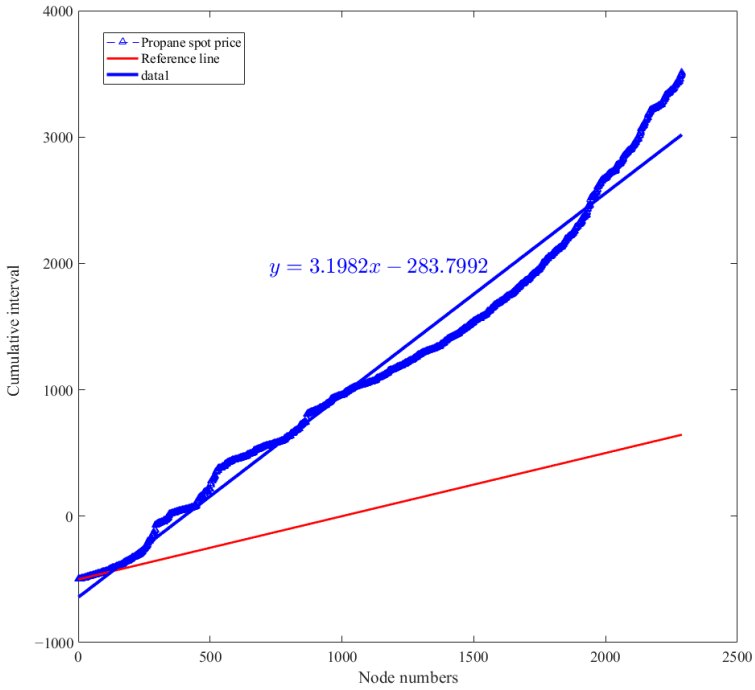


Figure 8. The cumulative time interval of new nodes appearing in the PPOWN.

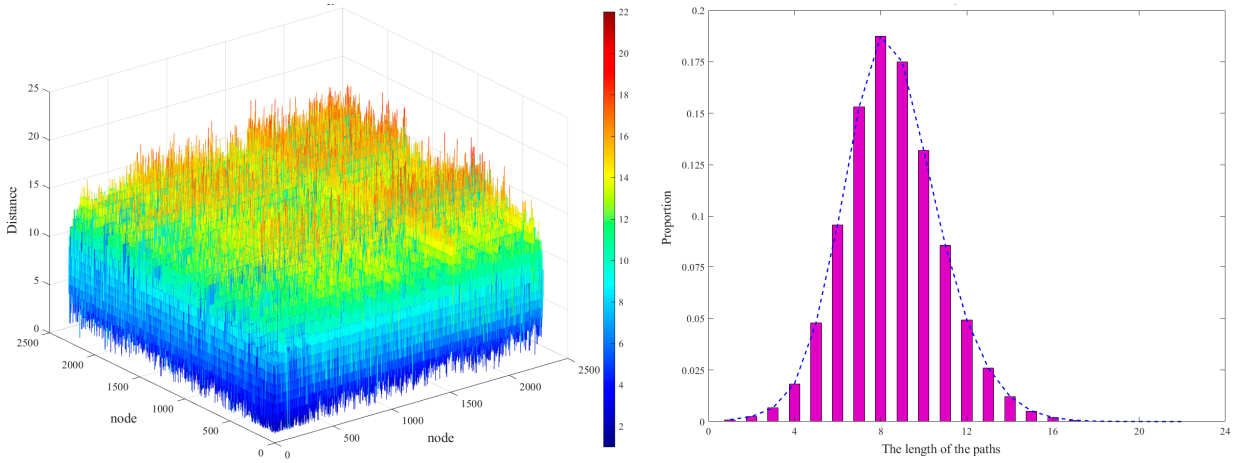
In Figure 8, the solid red line represents the curve of equal time intervals, in which it can be observed that, as time progresses, the intervals at which new nodes appear in the evolution of the PPOWN are not uniform; instead, they gradually increase, exhibiting a linear growth trend. Least squares regression analysis is conducted on the cumulative time of the new nodes appearing in the PPOWN. The resulting regression equation is denoted as $y = 3.1982x - 283.7992$, and its trend line correlation coefficient is represented as $R^2 = 0.9772$. The findings indicate a high degree of credibility, demonstrating that the cumulative time of the new nodes in the PPOWN exhibits a linear growth trend. This trend

is characterized by a consistent pattern, which reflects the predictability of the changes in the propane price based on the temporal distribution characteristics.

In summary, the emergence of new nodes in the PPOWN indicates the presence of abnormally fluctuating price nodes, which differ from previous fluctuations. Additionally, the cumulative duration of these abnormally fluctuating price nodes exhibits a linear growth trend. This pattern can be utilized to effectively identify the onset of the abnormally fluctuating price nodes, enabling price decision-makers to respond promptly to the new price fluctuations. Consequently, this approach enhances the accuracy of the propane price forecasts and mitigates price risks.

3.3. Conversion Cycle of the Nodes

According to Formulas (8) and (9), the distance between any two nodes in the PPOWN is calculated using the Floyd algorithm [33]. The results are presented in Figure 9a, while the distribution of various path lengths is illustrated in Figure 9b.



(**a**) (**b**)

Figure 9. (**a**) The distance and distribution between any two nodes in the PPOWN; (**b**) The proportion of the various path length in the PPOWN.

As illustrated in Figure 9, the diameter and average path length of the PPOWN are $D = 22$ and $\overline{L} = 8.4505$,respectively, but the distance between nodes ranges from 6 to 11, accounting for 82.86% of the total number of nodes; this indicates that the price fluctuation pattern in the PPOWN is predominantly short-range related, with a conversion cycle of the approximately 8 to 9 days, suggesting that conversions occur relatively frequently. This analytical result provides a theoretical foundation for predicting the periodic conversion patterns of propane prices in the future.

3.4. Betweenness of the Nodes

According to the definitions and formulas of the node betweenness in the network [35,36], the evolving relationship between the betweenness and strength of the nodes in the PPOWN over time is analyzed, as illustrated in Figure 10.

According to Figure 10, the betweenness of the nodes in the PPOWN, along with the strength, name, first appearance time, and location of their corresponding nodes, has been calculated. The nodes are then arranged in descending order based on their betweenness, as presented in Table 5, which includes only the top eight nodes.

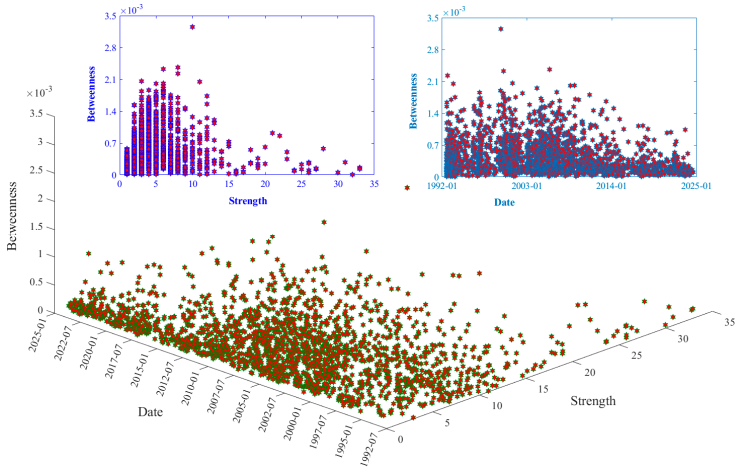


Figure 10. The relationship between the node betweenness and strength of the PPOWN over time.

Table 5. The betweenness, name, strength, initial appearance times, and location of their corresponding nodes in the PPOWN (only the top eight nodes).

Order	Betweenness	Name	Strength	Date	Location
1	0.003251858	rrRRf	10	12 August 1999	545th
2	0.002362096	frrRR	8	5 December 2005	1212th
3	0.002325613	RfrrR	6	15 December 1999	579th
4	0.002226625	rrrsf	8	11 September 1992	36th
5	0.002059869	RfrfF	3	12 February 2001	750th
6	0.002046589	rrrfs	11	11 June 1993	161st
7	0.002010586	FRrrR	6	26 February 2009	1537th
8	0.002005679	FFFRf	5	14 August 2008	1486th

According to Table 5, the relationship between the betweenness and strength of the node in the PPOWN reveals that nodes with a high betweenness exhibit low strength, which indicates that nodes with a lower strength play a crucial role in connecting the network. Their presence often signifies that the market has entered a transitional phase, which aligns with Borgatti's [40] theory on node betweenness centrality. The nodes with high strength are linked to other nodes through those with low betweenness. When the betweenness of the node is high and shows a continuous upward trend, it suggests that other nodes must pass through this node to connect with additional nodes, marking a significant period. Identifying these nodes during this phase can enable us to effectively predict the volatility of the propane price in the subsequent period.

3.5. Clustering Coefficient of the Nodes

This section primarily analyzes the evolutionary relationship between the clustering coefficient and strength of the node in the PPOWN with the time, which is shown in Figure 11.

The clustering coefficient quantifies the degree of aggregation among the nodes in a network and reflects the network's grouping characteristics. A higher clustering coefficient indicates a greater likelihood of pattern formation among the nodes. As illustrated in Figure 11, the clustering coefficient of the nodes 'sRRRR' and 'FRRRR' are both 0.5, which suggests a high likelihood that two nodes connected to the same node are also interconnected. This result suggests that there is a significant likelihood of the sharp rising state occurring in the future, at which point decision-makers are highly likely to develop effective strategies to cope with the propane price increases. According to the calculation result, the average clustering coefficient of the PPOWN is 0.0015. Notably, only 24 nodes

exhibit a clustering coefficient greater than zero, which are presented in the accompanying Table 6, arranged from largest to smallest.

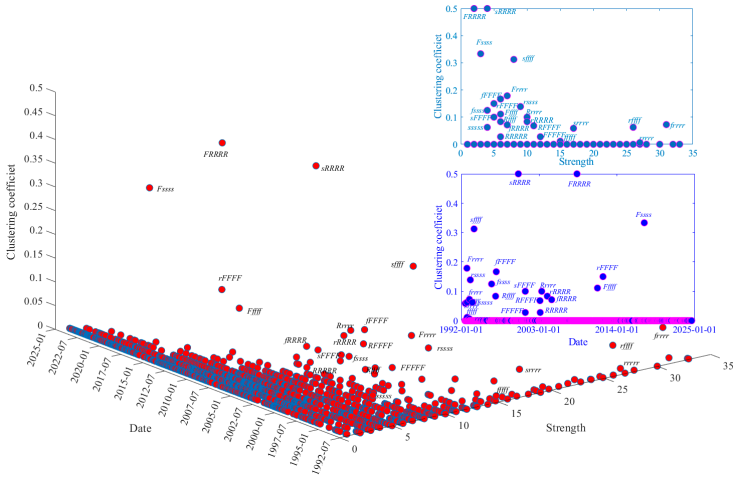


Figure 11. The evolutionary relationship between the clustering coefficient and strength of the node in the PPOWN over time.

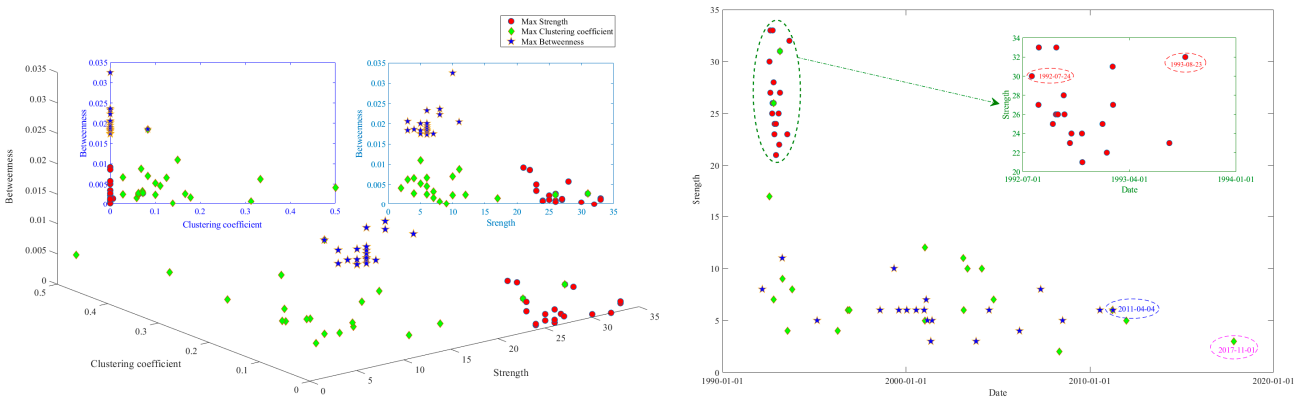
Table 6. The clustering coefficient, name, strength of the nodes in the PPOWN.

Order	Clustering Coefficient	Name	Strength	Order	Clustering Coefficient	Name	Strength
1	0.5000	sRRRR	4	13	0.0833	Rffff	6
2	0.5000	FRRRR	2	14	0.0833	rRRRR	10
3	0.3333	Fssss	3	15	0.0726	frrrr	31
4	0.3125	sffff	8	16	0.0714	fRRRR	7
5	0.1786	Frrrr	7	17	0.0682	RFFFF	11
6	0.1667	fFFFF	6	18	0.0625	rffff	26
7	0.1500	rFFFF	5	19	0.0625	sssss	4
8	0.1389	rssss	9	20	0.0588	srrrr	17
9	0.1250	fssss	4	21	0.0278	FFFFF	12
10	0.1111	‘Fffff’	6	22	0.0278	RRRRR	6
11	0.1000	sFFFF	5	23	0.0111	fffff	15
12	0.1000	Rrrrr	10	24	0.0062	rrrrr	27

By comparison, the clustering coefficient and average clustering coefficient of the PPOWN are both small, which indicates that the likelihood of two nodes, which are connected to a common node, also being connected to each other is minimal. Furthermore, the nodes with non-zero clustering coefficients in the PPOWN typically exhibit low strength, but a small subset of these nodes also demonstrates high strength, which suggests that the PPOWN is not entirely random and possesses certain characteristics of a “community” to some extent. However, the more pronounced clustering characteristics within its network may manifest in either small or large communities. The time distribution characteristics of the node clustering coefficient, which is not equal to zero, indicate that the clustering coefficient of the nodes in the PPOWN first emerged on 30 July 1992, and last appeared on 8 November 2017. The clustering coefficients may vary depending on the time scale, indicating that the volatility of propane prices can sometimes be observed on both larger and smaller time scales. Analyzing the clustering coefficient of the nodes in the PPOWN can provide valuable insights for future research on the clustering of the propane price fluctuations.

4. Comprehensive Analysis

In conjunction with the aforementioned analysis of the node strength, betweenness, and clustering coefficient in relation to the time distribution characteristics, the evolutionary relationships among these metrics are examined. Within the PPOWN, significant nodes exhibiting high values of node strength, betweenness, and clustering coefficient are identified. The evolutionary relationships among these nodes are illustrated in Figure 12a, while Figure 12b presents the time distribution characteristics of their initial appearances.



(**a**) (**b**)

Figure 12. (**a**) The evolutionary relationship among the max strength, max betweenness and max clustering coefficient in the PPOWN; (**b**) The time distribution characteristics of the initial appearances for the max strength, max betweenness and max clustering coefficient in the PPOWN.

It can be observed from Figure 12a that the PPOWN indicates a relationship where the nodes with a greater point strength tend to have lower betweenness and clustering coefficients. Conversely, the nodes exhibiting higher betweenness are associated with reduced node strength and clustering coefficients, while the nodes with elevated clustering coefficients demonstrate lower betweenness and point strength. Additionally, the emergence of nodes with significant node strength, betweenness, and clustering coefficients in the PPOWN is illustrated in Figure 12b. Notably, nodes with a high node strength (represented by "○" in the figure) first appeared predominantly between July 1992 and August 1993. It is evident that the nodes with high strength are often early nodes, while the nodes exhibiting greater betweenness (indicated by "☆" in the figure) are relatively dispersed, primarily concentrated between July 1992 and February 2011. The nodes with higher clustering coefficients (represented by "◇" in the figure) are the most scattered, with a concentration from July 1992 to November 2017, yet they still tend to appear early. The emergence of these nodes signifies that the propane price is in a fluctuating transitional stage. This fluctuation characteristic will aid in better understanding the patterns of the propane price changes.

5. Summaries and Insights

This paper utilizes the U.S. Energy Information Administration's propane spot prices from 9 July 1992 to 22 July 2024 as sample data and defines the fluctuation pattern through a coarse-grained method. We converted the fluctuation sequence of the propane price into a character string consisting of five symbols: {R, r, e, f, F}. Using a model with a duration of 5 days and a sliding step size of 1 day, we constructed a sliding window that can be obtained. In the corresponding propane price time series, the fluctuation modes are represented as the nodes in chronological order, while the transitions between the fluctuation modes serve as edges, with the number of transitions assigned as weights, then the PPOWN is established.

According to the PPOWN, we then analyzed the evolution of new nodes appearing in the PPOWN. We calculated the strength, strength distribution, clustering coefficients, and the average shortest path of the PPOWN, identifying important nodes and their occurrence times. The results are as follows:

(1) Through the analysis of the strength and distribution of nodes in the PPOWN, we find that the core fluctuation state is represented by the first 0.96% of nodes, the average contribution rate of the interconnections among the important nodes is 55.77%. Most nodes exhibit low strength, while only a few possess high strength, which is a characteristic feature of scale-free networks. Additionally, the connections between the nodes with high strength are very close. However, while the nodes with high strength tend to be those that appeared earlier, it is not necessarily the case that the earlier nodes possess high strength.

(2) According to the Floyd algorithm, the distance between any two nodes is calculated to determine the average path length in the PPOWN. The results indicate that the fluctuation mode conversion period of the PPOWN is 8 to 9 days, which suggests a short-range correlation between the price fluctuation modes within the PPOWN, as well as the complexity and diversity of its price fluctuation states.

(3) Although propane price fluctuations exhibit complex nonlinearity, the cumulative times when the new nodes appear in the PPOWN is not nonlinear. Through the analysis of the regularity in the emergence of new nodes within the PPOWN, it was discovered that the cumulative time for the emergence of the new nodes exhibited a strong linear growth trend. This result is beneficial for predicting both the emergence of new nodes and the time of their corresponding appearance in the network.

(4) The PPOWN indicates that nodes with low strength have a considerable ability to influence communication among other nodes. The presence of these low-strength nodes suggests that the network is undergoing a transitional phase. Identifying and analyzing these nodes can effectively predict the fluctuation of the propane price in the upcoming period. Through the examination of the network's clustering effect, it has been observed that certain nodes can serve as the shortest path between other pairs of nodes within the entire network. This result offers valuable insights and guidance for future studies on the clustering of the propane price. Finally, through a comprehensive analysis of the strength, betweenness, and clustering coefficient for the node in relation to the time distribution characteristics, it was found that the PPOWN exhibits a low betweenness, clustering coefficients, and strength for the node. This behavior is distinct from that of random and chaotic networks.

The propane market price is influenced by various factors, including market demand, supply levels, fluctuations in crude oil prices, geopolitical events, seasonal variations, macroeconomic conditions, changes in the financial markets, the policy environment, and transportation and logistics conditions. Together, these factors determine the trends and levels of propane price fluctuations, making the study of these characteristics highly valuable in practical terms. Therefore, the research presented in this paper offers theoretical support for various participants in the energy market to forecast future propane price trends within the context of overarching market dynamics. This has significant implications for understanding systemic risk behaviors in the energy market and for informing investment strategies within this sector. On the one hand, future research will focus on constructing a multi-level interdependent network model driven by the multi-factor synergy, and this model aims to elucidate the core mechanisms of the price transmission among various factors, and it will integrate the patterns of the new node emergence with the identification of key nodes to predict the states of the nodes. On the other hand, future research will concentrate on developing a multi-level interdependent network model driven by synergistic interactions among multiple factors, and this model will aim to clarify the fundamental

mechanisms of price transmission across various elements. Meanwhile, it will incorporate the patterns of new node emergence while identifying key nodes to forecast the states of network nodes.

Author Contributions: Conceptualization, G.Z., J.Y. and Z.Q.; methodology, G.Z. and J.Y.; software, G.Z. and Y.Z.; validation, G.Z., Y.Z. and Z.Q.; formal analysis, G.Z.; investigation, G.Z.; resources, J.Y. and Y.Z.; data curation, G.Z.; writing—original draft preparation, G.Z. and Z.Q.; writing—review and editing, G.Z. and J.Y.; visualization, G.Z. and Y.Z.; supervision, Z.Q.; project administration, Z.Q.; funding acquisition, G.Z. and Z.Q. All authors have read and agreed to the published version of the manuscript.

Funding: This research is supported by the Shandong Provincial Natural Science Foundation (N (Grant No. ZR2021MF133, Grant No. ZR2022MF278), the National Natural Science Foundation of China (Grant No. 72174091), "Taihu Light" Science and Technology Project of Wuxi (Grant No. K20231036) and Wuxi University Research Start-up Fund for Introduced Talents (Grant No. 2023r046).

Data Availability Statement: The original data presented in the study are openly available in [Petroleum & Other Liquids] at [https://www.eia.gov/dnav/pet/pet_pri_spt_s1_d.htm] (Accessed on 28 July 2024).

Conflicts of Interest: The authors declare no conflicts of interest.

References

1. Abakah, E.J.A.; Shao, D.X.; Tiwari, A.K.; Lee, C.C. Asymmetric relationship between carbon market and energy markets. *Energy* **2024**, *313*, 133656. [CrossRef]
2. Ayinde, T.O.; Adeyemi, F.A. Fossil fuel prices and economic policy uncertainty–A regime-switching approach. *Energy Clim. Change* **2024**, *5*, 100140. [CrossRef]
3. Lahmiri, S. Fossil energy market price prediction by using machine learning with optimal hyper-parameters, A comparative study. *Resour. Policy* **2024**, *92*, 105008. [CrossRef]
4. Hamilton, J.D. *Time Series Analysi*; Princeton University Press: Princeton, NJ, USA, 1994.
5. Pindyck, R.S. Volatility and commodity price dynamics. *J. Futures Mark.* **2004**, *24*, 1029–1047. [CrossRef]
6. Dias, J.G.; Ramos, S.B. Energy price dynamics in the US market. Insights from a heterogeneous multi-regime framework. *Energy* **2014**, *68*, 327–336. [CrossRef]
7. Kim, S.; Jeong, S.; Heo, E. Effects of the shale boom on ethylene and propylene prices. *Energy Sources Part B Econ. Plan. Policy* **2019**, *14*, 49–66. [CrossRef]
8. Nazlioglu, S.; Soytas, U.; Gupta, R. Oil prices and financial stress: A volatility spillover analysis. *Energy Policy* **2015**, *82*, 278–288. [CrossRef]
9. Moul, C.C.; Miller, B.A. An aggregate test for transient market power in the winter 2013–14 propane market. *Econ. Lett.* **2021**, *200*, 109765. [CrossRef]
10. Zhang, Y.J.; Wang, Z.Y. Investigating the price discovery and risk transfer functions in the crude oil and gasoline futures markets: Some empirical evidence. *Appl. Energy* **2013**, *104*, 220–228. [CrossRef]
11. Hung, N.T. Identifying the dynamic connectedness between propane and oil prices, Evidence from wavelet analysis. *Int. J. Energy Econ. Policy* **2020**, *10*, 315–326. [CrossRef]
12. Wang, X.T.; Fang, F.; Ma, S.Q.; Xiang, L.J.; Xiao, Z.M. Dynamic volatility spillover among cryptocurrencies and energy markets: An empirical analysis based on a multilevel complex network. *North Am. J. Econ. Financ.* **2024**, *69*, 102035. [CrossRef]
13. Chen, W.; Xiong, S.; Chen, Q. Characterizing the dynamic evolutionary behavior of multivariate price movement fluctuation in the carbon-fuel energy markets system from complex network perspective. *Energy* **2022**, *239*, 121896. [CrossRef]
14. Chiroma, H.; Abdul-Kareem, S.; Gital, A.Y.; Muaz, S.A.; Herawan, T. An ensemble CRT, RVFLN, SVM method for estimating propane spot price. *Adv. Intell. Syst. Comput.* **2015**, *331*, 21–30.
15. Emmert-Streib, F.; Dehmer, M. Networks for systems biology, conceptual connection of data and function. *IET Syst. Biol.* **2012**, *6*, 63–69. [CrossRef]
16. Mantegna, R.N.; Stanley, H.E. *Introduction to Econophysics, Correlations and Complexity in Finance*; Cambridge University Press: New York, NY, USA, 1999.
17. Huang, C.; Cai, Y.; Cao, J.; Deng, Y. Stock complex networks based on the GA-LightGBM model: The prediction of firm performance. *Inf. Sci.* **2025**, *700*, 121824. [CrossRef]
18. He, L.Y.; Chen, S.P. Crude oil price analysis and forecasting based on complex network theory. *Energy Econ.* **2020**, *91*, 104878.

19. Criado-Ramón, D.; Ruíz, L.G.B.; Pegalajar, M.C. Electric demand forecasting with neural networks and symbolic time series representations. *Appl. Soft Comput.* **2022**, *122*, 108871. [CrossRef]
20. Narayan, P.K.; Narayan, S.; Popp, S. Investigating price clustering in the oil futures market. *Appl Energy* **2011**, *88*, 397–402. [CrossRef]
21. Daw, C.S.; Finney, C.E.; Tracy, E.R. A review of symbolic analysis of experimental data. *Rev. Sci. Instrum.* **2003**, *74*, 915–930. [CrossRef]
22. Wu, J.; Xu, K.; Chen, X.; Li, S.; Zhao, J. Price graphs: Utilizing the structural information of financial time series for stock prediction. *Inf. Sci.* **2021**, *587*, 618–633. [CrossRef]
23. Zhou, R.; Cai, R.; Tong, G. Applications of symbolic dynamics in economic time series analysis. *Phys. A Stat. Mech. Its Appl.* **2017**, *482*, 658–668.
24. Cheng, D.; Yang, F.; Xiang, S.; Liu, J. Financial time series forecasting with multi-modality graph neural network. *Pattern Recognit.* **2021**, *120*, 108218. [CrossRef]
25. Izati, P.P.; Prastyo, D.D.; Akbar, M.S. Modeling the Volatility of World Energy Commodity Prices Using the GARCH-Fractional Cointegration Model. *Procedia Comput. Sci.* **2024**, *234*, 412–419. [CrossRef]
26. Chen, L.; Pan, L.; Zhang, K. The Dynamic Cointegration Relationship between International Crude Oil, Natural Gas, and Coal Price. *Energies* **2024**, *17*, 3126. [CrossRef]
27. Wang, M.G.; Tian, L.X.; Zhou, P. A novel approach for oil price forecasting based on data fluctuation network. *Energy Econ.* **2018**, *71*, 201–212. [CrossRef]
28. Chen, H.; Tian, L.X.; Wang, M.G.; Zhen, Z.L. Analysis of the Dynamic Evolutionary Behavior of American Heating Oil Spot and Futures Price Fluctuation Networks. *Sustainability* **2017**, *9*, 574. [CrossRef]
29. Choi, I.; Kim, W.C. Estimating historical downside risks of global financial market indices via inflation rate-adjusted dependence graphs. *Res. Int. Bus. Financ.* **2023**, *65*, 102077. [CrossRef]
30. Gao, X.Y.; An, H.Z.; Liu, H.H.; Ding, Y.H. Analysis on the topological properties of the linkage complex network between crude oil future price and spot price. *Acta Phys. Sin.* **2011**, *60*, 843–852.
31. An, H.Z.; Gao, X.Y.; Fang, W.; Ding, Y.H.; Zhong, W.Q. Research on patterns in the fluctuation of the co-movement between crude oil futures and spot prices, A complex network approach. *Appl. Energy* **2014**, *136*, 1067–1075. [CrossRef]
32. Yang, Y.; Poon, J.P.; Liu, Y.; Bagchi-Sen, S. Small and flat worlds: A complex network analysis of international trade in crude oil. *Energy* **2015**, *93*, 534–543. [CrossRef]
33. Geng, J.B.; Ji, Q.; Fan, Y. A dynamic analysis on global natural gas trade network. *Appl. Energy* **2014**, *132*, 23–33. [CrossRef]
34. Watts, D.J.; Strogatz, S.H. Collective dynamics of "small-world" networks. *Nature* **1998**, *393*, 440–442. [CrossRef] [PubMed]
35. Wang, M.G.; Chen, Y.; Tian, L.X.; Jiang, S.M.; Tian, Z.H.; Du, R.J. Fluctuation behavior analysis of international crude oil and gasoline price based on complex network perspective. *Appl. Energy* **2016**, *175*, 109–127. [CrossRef]
36. Freeman, L.C. A set of measures of centrality based on betweenness. *Sociometry* **1977**, *40*, 35–41. [CrossRef]
37. Brandes, U. A faster algorithm for betweenness centrality. *J. Math. Sociol.* **2001**, *25*, 163–177. [CrossRef]
38. Chen, W.D.; Xu, H.; Guo, Q. Dynamic analysis on the topological properties of the complex network of international oil prices. *Acta Phys. Sin.* **2010**, *59*, 4514–4523. [CrossRef]
39. Wei, D.H. An Optimized Floyd Algorithm for the Shortest Path Problem. *J. Netw.* **2010**, *5*, 1496–1504. [CrossRef]
40. Borgatti, S.P. Centrality and network flow. *Soc. Netw.* **2005**, *27*, 55–71. [CrossRef]

Disclaimer/Publisher's Note: The statements, opinions and data contained in all publications are solely those of the individual author(s) and contributor(s) and not of MDPI and/or the editor(s). MDPI and/or the editor(s) disclaim responsibility for any injury to people or property resulting from any ideas, methods, instructions or products referred to in the content.